■Ngày nhận bài: 07/12/2023 ■Ngày sửa bài: 08/01/2024 ■Ngày chấp nhận đăng: 05/02/2024

Design of NATM tunnel by 3D numerical simulations and analytical method

Thiết kế đường hầm NATM bằng phương pháp mô phỏng 3D và phân tích

> PH.D CONG GIANG NGUYEN
Lecturer, Construction Faculty, Hanoi Architectural University
Email: gianglientca@gmail.com

ABSTRACT

NATM (New Austrian Tunneling Method) has been widely used in Vietnam for road tunnel construction through the mountains. The main feature of NATM is to utilize all available means to develop the maximum self-supporting capacity of the surrounding rock or soil itself and to undertake investigation and monitoring during construction to provide stability to the tunnel. Tunnel excavation adopting the NATM is usually divided into sub-sections to be excavated in sequential steps. The application of temporary reinforcements then follows the whole of each subsection. Different unsupported span lengths in the longitudinal direction at each step considerably affect stress redistribution in the ground, soil deformation, and stress-induced tunnel support systems. This study simulates a mountain road tunnel using finite element analyses. The numerical calculations will be obtained and discussed to predict ground deformation stress changes around the tunnel opening and final displacements in each construction stage.

Keywords: NATM; self-supporting capacity; finite element analyses; stress; soil deformation; numerical modeling; final displacements.

1. INTRODUCTION

The escalating demand for tunnels in urban areas, primarily fueled by the exorbitant cost of urban space, has underscored the need for efficient tunnel excavation methods. While traditional approaches like shields and tunnel boring machines have demonstrated effectiveness, they may lack the necessary flexibility to accommodate diverse tunnel geometries. In response, the New Austrian Tunnelling Method (NATM) has emerged as a flexible alternative, capable of adapting to different soil conditions. NATM is grounded in three fundamental principles: treating the soil as an active structure component, optimizing tunnel lining to control deformation, and incorporating instrumentation for adaptive design.

Despite the reliance on empirical knowledge in NATM, there is a discernible shift towards integrating numerical analyses, particularly leveraging the finite element method (FEM), into tunnel design processes. Although 2-D FEM analyses are widely used, it is increasingly recognized that tunnel excavation induces a 3-D stress and strain field, necessitating 3-D simulations for accurate evaluations, especially in scenarios involving ground reinforcement techniques.

However, adopting 3-D simulations presents computational challenges, demanding substantial resources. Developers are focusing on creating efficient iterative solvers to overcome this hurdle. The literature reflects a rising prevalence of 3-D analyses, with ongoing projects aiming to incorporate computer-based numerical simulation tools into tunnel design methodologies. These projects explore various techniques, including FEM, finite difference method (FDM), boundary element method (BEM), and distinct element method (DEM).

In addition to examining the challenges associated with 3-D simulations, the paper discusses their benefits for tunnels excavated using diverse methods, such as shields, tunnel boring machines, and the innovative Umbrella Method. The latter involves drilling long steel pipes around the tunnel periphery and utilizing grouting to stabilize the tunnel crown and cutting face, thereby minimizing ground settlements. The study employs numerical analyses to simulate and evaluate settlement control techniques in NATM tunnel excavation, encompassing strategies like partial-face excavation, free span distance adjustments, and the activation of additional support measures.

2. NUMERICAL APPROXIMATIONS

A series of 3-D simulations using the finite element method were performed to investigate the influence of the following aspects: (a) unsupported distance between the excavation face and the installation of support lining; (b) partial-face excavation; (c) closure of invert arc and full activation of support.

The tunnel model is simulated using MIDAS software. Several new aspects were added to the program to facilitate 3-D analyses of tunnel excavation. Excavated elements are deactivated from the mesh, internally renumbered, and optimized by the program. Stresses in the excavated elements are converted into forces along the excavation boundary at each stage, representing the construction advance. These forces may be incrementally applied at each stage, and the size of the increments is either fixed by the user or automatically computed by the program. Different non-linear solution schemes are available, and a choice of constitutive models is also implemented. Reactivating elements in the lining area simulates tunnel lining with a new constitutive model and material properties.

The 3-D finite element mesh used in the present analyses is shown in Fig. 1. The tunnel has a bottom width of 22m and a tunnel height of 14.75m, and the tunnel passes through 3 types of geology: weathered rock, soft rock, and bedrock.

As the main focus of these analyses was to establish the relative effectiveness of different construction techniques in reducing surface settlements, a simple elastic linear model was adopted for the soil mass and concrete lining. The authors recognize, however, that for proper quantitative and qualitative prediction of ground movements, a more appropriate constitutive model is of paramount importance. However, the relative importance of the factors investigated here with the elastic linear model is expected to hold for more sophisticated constitutive relations.

An elastic modulus (E) of 4.9 GPa with a coefficient of Poisson (m) of 0.2 for the concrete lining was adopted. The elastic modulus for the weathered rock was 84 MPa with a coefficient of Poisson equal to 0.35. This last parameter is compatible with a coefficient of earth pressure at rest (K0) equal to 1. The value of the unity weight of the soil of 18 kN/m3 was used to generate the initial geostatic stress state. Similarly, soft rock and bedrock values are 250 MPa and 2767 MPa for elastic modulus and 0.3 and 0.25 for Poisson's coefficient, respectively. The coefficient of earth pressure at rest (K0) is equal to 1; The value of unity weight is 20kN/m3 and 25.7kN/m3, respectively.

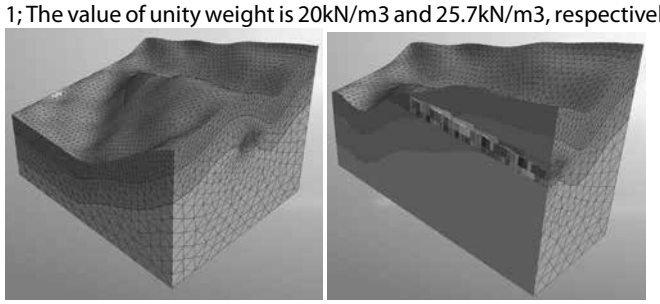

Figure 1. Three-dimensional finite element mesh

Table 1. Geotechnical properties of soil layers input the software

Name	Weathered Soil	Soft rock	Bed rock	Reinforced Zone
Material	Isotropic	Isotropic	Isotropic	Isotropic
General	Mohr Coulomb	Mohr Coulomb	Mohr Coulomb	Mohr Coulomb
Elastic Modulus (E) (KN/m^2)	84000	250266	2767000	1470997.5
Poisson's Ratio (v)	0.35	0.3	0.25	0.3
Unit Weight kN/m^3	18	19	25.7	19.61
K_0	1	1	1	1
Unit Weight (Saturated) kN/m^3	19	20	25.7	21.6
Initial Void Ratio (e_0)	0.5	0	0	0
Drainage Parameters	Drained	Drained	Drained	Drained
Cohesion (C)	65	100	670	588.4
Frictional Angle	34	43.8	58	30

Table 2. Technical specifications of Tunnel Lining, Rockbolt, Pipe umbrella

Name	Soft Shotcrete (Soft S/C)	Rockbolt	Pipe umbrella
Material	Isotropic	Isotropic	Isotropic
General	Elastic	Elastic	Elastic
Elastic Modulus (E) (KN/m^2)	4,9E+06	206E+06	206E+06
Poisson's Ratio (v)	0.2	0.3	0.3
Unit Weight kN/m^3	23.54	76.98	76.98

Table 3. Property of material

Name	Weathered Soil	Soft rock	Bed rock	Reinforced Zone	Soft Shotcrete (Soft S/C)	Rockbolt	Pipe umbrella
Type	3D	3D	3D	3D	2D	1D	1D
Sub-Type	Solid	Solid	Solid	Solid	Shell	Embedded Beam	Beam
Cross Section Area (A)	-	-	-	-	-	-	0.00135698613
Torsional Constant (Ix)	-	-	-	-	-	-	9.486574e-007
Torsional Stress Coeff							0.03025
Area Moment of Inertia (Iy)							4.743287e-007
Area Moment of Inertia (Iz)							4.743287e-007
Effective Shear Area (Ay)							0.000678493064
Effective Shear Area (Az)							0.000678493064
Shear Stresss Coefficient (Gy)							1449.82295
Shear Stresss Coefficient (Gz)							1449.82295

3. PRELIMINARY ANALYSIS

A given cross-section may be divided into smaller regions, as in Fig. 2(a). NATM tunnel consists of tunnel lining, upper reinforcement area, and two side anchors. To illustrate the 3-D excavation, all regions of a cross-section are schematically depicted in the convention shown in Fig. 2(b). Each advance is 4m, and the digging process is divided into 2 parts, digging above first and digging below later.

The tunneling construction process is simulated sequentially in several stages. Each construction stage may involve soil excavation

and support lining construction along one or more longitudinal segments. In a given longitudinal segment, soil excavation may be simulated in full-face, when all elements are deactivated in one simulation stage, or partial-face excavation with regions sequentially deactivated in several stages. Similarly, support construction in one segment may be complete or partial. The free distance between the excavation face and the support heading will be called the free span (L1). The support is fully activated only when the whole concrete arc is constructed. The gap between the excavation face and the first lining section will be called the total support distance (L2). Each time the excavation face moves, one section forward will be referred to as a tunnel advance.

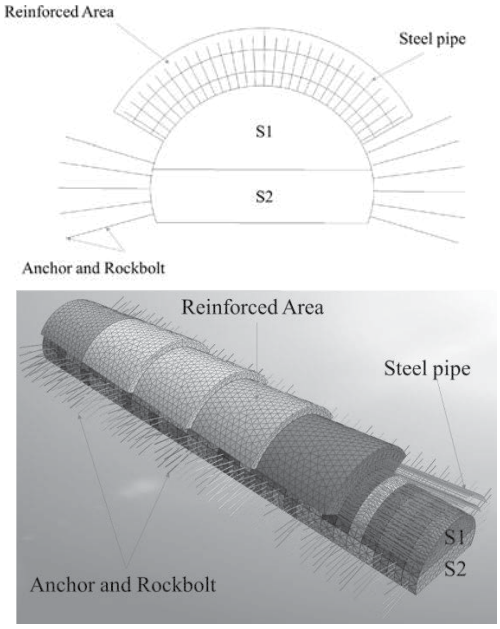

Figure 2. Cross-section and simulation model of NATM tunnel

The construction phase described in Figure 3 is the construction of a steel pipe umbrella to create a reinforced area. Excavation of 4m of soil in area S1 will begin. After excavating the soil in area S1, construct the upper tunnel lining and create anchors into the rock to fix the tunnel lining and make the tunnel lining and rock support the tunnel. At the same time, dig another 4m of soil in the area S1. Then, construct the second tunnel lining and anchors simultaneously, excavate the next 4m of S1 soil and the first 4m of area S2 soil, and build the lower tunnel lining combined with rock anchors. Continue like this sequentially until the tunnel is completed. In this case, more than one set of longitudinal schematic segments would be necessary to illustrate the complete 3-D process.

A few initial analyses were made to emphasize a few isolated effects, such as (a) the 3-D stress distribution, (b) the importance of support installation, and (c) the importance of partial-face excavation.

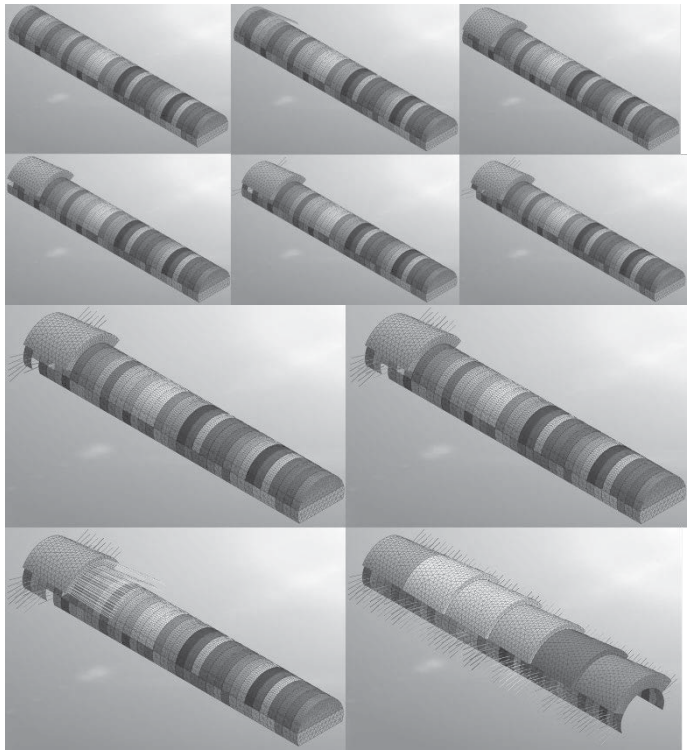

Figure 3. The NATM tunnel construction process is simulated using GTS NX software

Unlike the TBM tunnel construction method, it is necessary to simulate many types of loads acting on the tunnel lining as well as on the drilling pressure loads, Jack thrust loads, shield external pressure loads, and segment external pressure loads. Tunnel lining: when constructing a tunnel using the NATM method, only the self-load of rock and soil acts on the tunnel.

Set type	Set name Prefix	I.S.	S1	S2	S3	S4	S5	S6	S7	S8	S9	S10	S11	S12	S13	S14	S15	S16	S17	S18	S19	S20
Mesh set	bed rock	A: -																				
Mesh set	bottom r/b #-								A: 1	A: 2	A: 3	A: 4	A: 5	A: 6	A: 7	A: 8	A: 9	A: 10	A: 11	A: 12	A: 13	A: 14
Boundary Set	bottom s/c-									A: 1	A: 2	A: 3	A: 4	A: 5	A: 6	A: 7	A: 8	A: 9	A: 10	A: 11	A: 12	A: 13
Mesh set	bottom s/c-								A: 1	A: 2	A: 3	A: 4	A: 5	A: 6	A: 7	A: 8	A: 9	A: 10	A: 11	A: 12	A: 13	A: 14
Mesh set	bottom tunnel #-	A: 1to36						R: 1	R: 2	R: 3	R: 4	R: 5	R: 6	R: 7	R: 8	R: 9	R: 10	R: 11	R: 12	R: 13	R: 14	R: 15
Boundary Set	boudnary	A: -																				
Mesh set	Default Mesh Set																					
Mesh set	excavaction	A: -		R: -																		
Load Set	gravity	A: -																				
Boundary Set	pipe 1 fixed				A: -																	
Boundary Set	pipe 2 fixed										A: -											
Boundary Set	pipe 3 fixed																A: -					
Boundary Set	pipe 4 fixed																					
Boundary Set	pipe 5 fixed																					
Boundary Set	pipe 6 fixed																					
Mesh set	soft rock	A: -																				
Mesh set	top r/b #-						A: 1	A: 2	A: 3	A: 4	A: 5	A: 6	A: 7	A: 8	A: 9	A: 10	A: 11	A: 12	A: 13	A: 14	A: 15	A: 16
Boundary Set	top s/c-						A: 1	A: 2	A: 3	A: 4	A: 5	A: 6	A: 7	A: 8	A: 9	A: 10	A: 11	A: 12	A: 13	A: 14	A: 15	A: 16
Mesh set	top s/c-						A: 1	A: 2	A: 3	A: 4	A: 5	A: 6	A: 7	A: 8	A: 9	A: 10	A: 11	A: 12	A: 13	A: 14	A: 15	A: 16
Mesh set	top tunnel #-	A: 1to36				R: 1	R: 2	R: 3	R: 4	R: 5	R: 6	R: 7	R: 8	R: 9	R: 10	R: 11	R: 12	R: 13	R: 14	R: 15	R: 16	R: 17
Mesh set	umbrella	A: 1to6																				
Boundary Set	umbrella				A: 1						A: 2						A: 3					
Mesh set	umbrella 1_Interior Edge				A: -																	
Mesh set	umbrella 2_Interior Edge										A: -											
Mesh set	umbrella 3_Interior Edge																A: -					
Mesh set	umbrella 4_Interior Edge																					
Mesh set	umbrella 5_Interior Edge																					
Mesh set	umbrella 6_Interior Edge																					
Mesh set	weathered soil	A: -																				

S21	S22	S23	S24	S25	S26	S27	S28	S29	S30	S31	S32	S33	S34	S35	S36	S37	S38	S39	S40	S41	S42	S43
A: 15	A: 16	A: 17	A: 18	A: 19	A: 20	A: 21	A: 22	A: 23	A: 24	A: 25	A: 26	A: 27	A: 28	A: 29	A: 30	A: 31	A: 32	A: 33	A: 34	A: 35	A: 36	
A: 14	A: 15	A: 16	A: 17	A: 18	A: 19	A: 20	A: 21	A: 22	A: 23	A: 24	A: 25	A: 26	A: 27	A: 28	A: 29	A: 30	A: 31	A: 32	A: 33	A: 34	A: 35	A: 36
A: 15	A: 16	A: 17	A: 18	A: 19	A: 20	A: 21	A: 22	A: 23	A: 24	A: 25	A: 26	A: 27	A: 28	A: 29	A: 30	A: 31	A: 32	A: 33	A: 34	A: 35	A: 36	
R: 16	R: 17	R: 18	R: 19	R: 20	R: 21	R: 22	R: 23	R: 24	R: 25	R: 26	R: 27	R: 28	R: 29	R: 30	R: 31	R: 32	R: 33	R: 34	R: 35	R: 36		
A: -																						
						A: -																
												A: -										
A: 17	A: 18	A: 19	A: 20	A: 21	A: 22	A: 23	A: 24	A: 25	A: 26	A: 27	A: 28	A: 29	A: 30	A: 31	A: 32	A: 33	A: 34	A: 35	A: 36			
A: 16	A: 17	A: 18	A: 19	A: 20	A: 21	A: 22	A: 23	A: 24	A: 25	A: 26	A: 27	A: 28	A: 29	A: 30	A: 31	A: 32	A: 33	A: 34	A: 35	A: 36		
A: 17	A: 18	A: 19	A: 20	A: 21	A: 22	A: 23	A: 24	A: 25	A: 26	A: 27	A: 28	A: 29	A: 30	A: 31	A: 32	A: 33	A: 34	A: 35	A: 36			
R: 18	R: 19	R: 20	R: 21	R: 22	R: 23	R: 24	R: 25	R: 26	R: 27	R: 28	R: 29	R: 30	R: 31	R: 32	R: 33	R: 34	R: 35	R: 36				
A: 4						A: 5						A: 6										
A: -																						
						A: -																
												A: -										

Figure 4. Tunnel construction stages

4 RESULT

4.1. DISPLACEMENT

4.1.1. Soil displacement

Table 4. Maximum displacement value of soil at each construction stage

Stage	Node	Maximum (m)	Stage	Node	Maximum (m)
I.S.	955	0.00E+00	S22	500	5.74E-02
null	955	0.00E+00	S23	500	5.76E-02
exca	32726	4.42E-02	S24	500	5.79E-02
S3	32726	4.42E-02	S25	500	5.82E-02
S4	32707	4.47E-02	S26	500	5.84E-02
S5	32707	4.58E-02	S27	500	5.86E-02
S6	32707	4.84E-02	S28	500	5.88E-02
S7	32707	4.98E-02	S29	500	5.90E-02
S8	32707	5.07E-02	S30	500	5.92E-02
S9	32707	5.11E-02	S31	500	5.93E-02
S10	32707	5.14E-02	S32	500	5.94E-02
S11	32707	5.16E-02	S33	500	5.96E-02
S12	14	5.32E-02	S34	500	5.98E-02
S13	14	5.45E-02	S35	500	5.99E-02
S14	14	5.54E-02	S36	500	5.99E-02
S15	500	5.59E-02	S37	500	6.00E-02
S16	500	5.62E-02	S38	500	6.00E-02
S17	500	5.63E-02	S39	501	6.01E-02
S18	500	5.65E-02	S40	501	6.01E-02
S19	500	5.67E-02	S41	501	6.01E-02
S20	500	5.69E-02	S42	501	6.01E-02
S21	500	5.72E-02	S43	501	6.01E-02

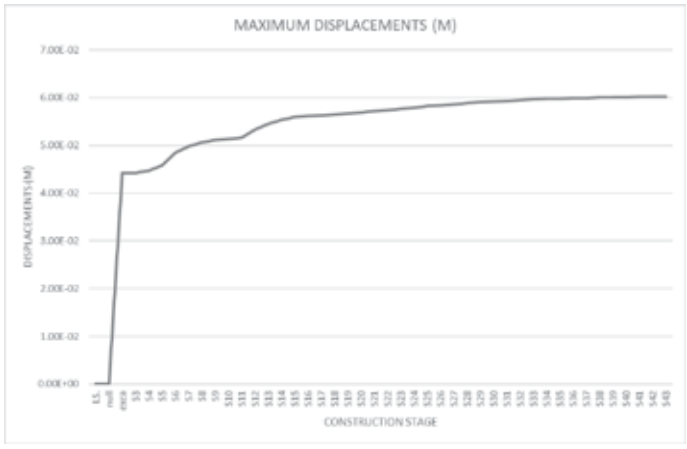

Figure 5. Chart of maximun displacements of soil at each construction stage

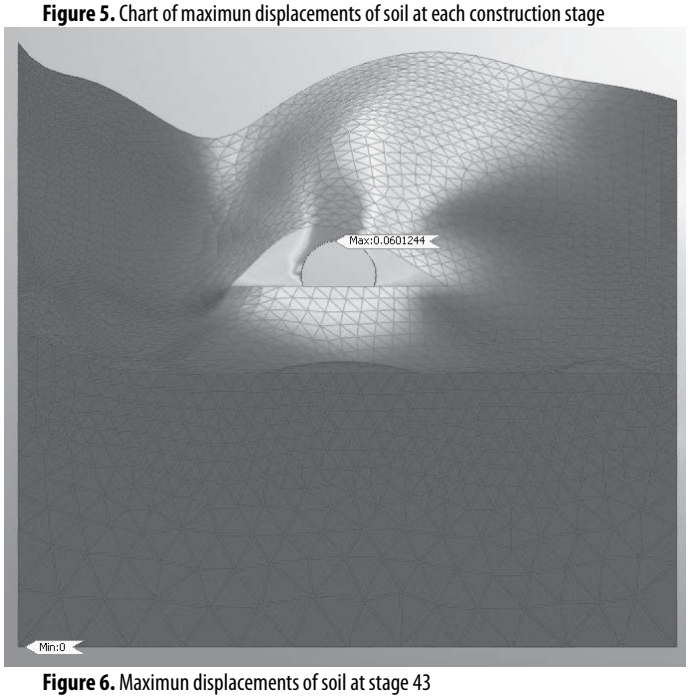

Figure 6. Maximun displacements of soil at stage 43

The largest displacement occurs at the intersection between the tunnel lining and rock because when excavating, a void will be created, and the soil above the tunnel will lose its natural support, leading to displacement under the influence of self-loading because soil and rock must redistribute to stabilize itself. This is overcome by constructing a steel pipe umbrella before digging to create a reinforcement area to prevent movement as well as enhance the self-stabilization ability of the soil and rock above the tunnel.

The maximum displacement reached a value of 6.012cm at the 43rd construction stage (S43) at the tunnel entrance. Because this area has a thin overburden of cover and a small cross-sectional area, when you go deeper, the overburden is thicker, and the soil and rock are more stable, so the displacement also gradually decreases.

4.1.2. Displacement of tunnel crown

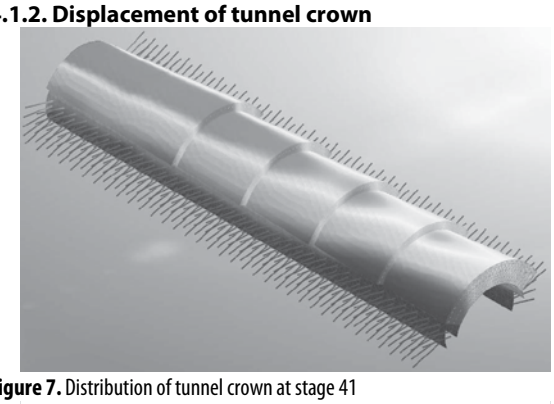

Figure 7. Distribution of tunnel crown at stage 41

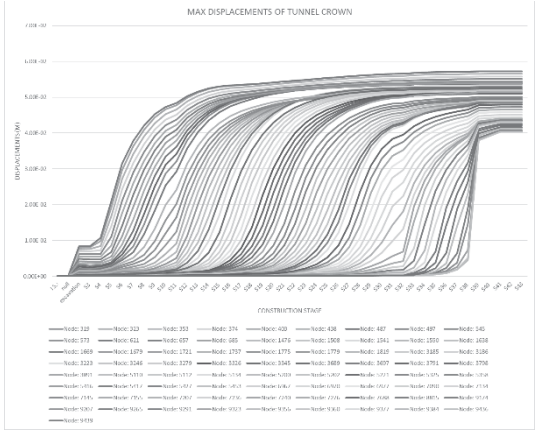

Figure 8. Chart of displacements of tunnel crown along the tunnel

Displacement of the tunnel crown is determined at points along the tunnel length. The chart shows that the maximum displacement of the tunnel crown is 0.05727078m (=5.7cm) at node 497 at the 41st construction stage.

4.2. FORCES AND MOMENTS IN STRUCTURAL MEMBERS

4.2.1. Anchor

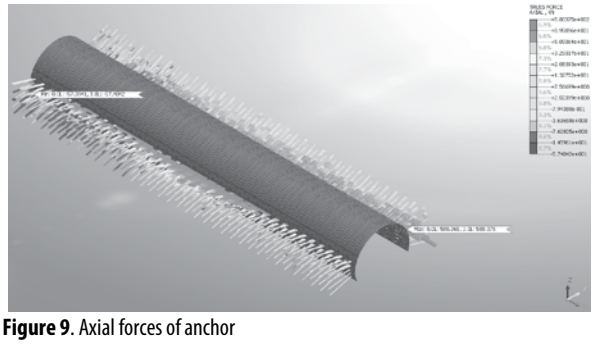

Figure 9. Axial forces of anchor

During tunnel construction using the NATM method, the maximum and minimum axial forces of the truss are not only located in the section with the most unfavorable geology but change according to the construction stage's different cross-sectional positions. So, when designing a NATM tunnel, we need to take the maximum axial forces value that appears during the construction phase as the initial calculation and design value.

The maximum axial force value of the anchors is 580.375 kN at construction stage 43 (S43)

Because the anchors is perpendicular to the tunnel lining, it plays a role in maintaining the stability of the surrounding rock and soil environment and the tunnel and is only affected by traction force. So, in this simulation, there is no torque.

4.2.2. Steel pipe umbrella

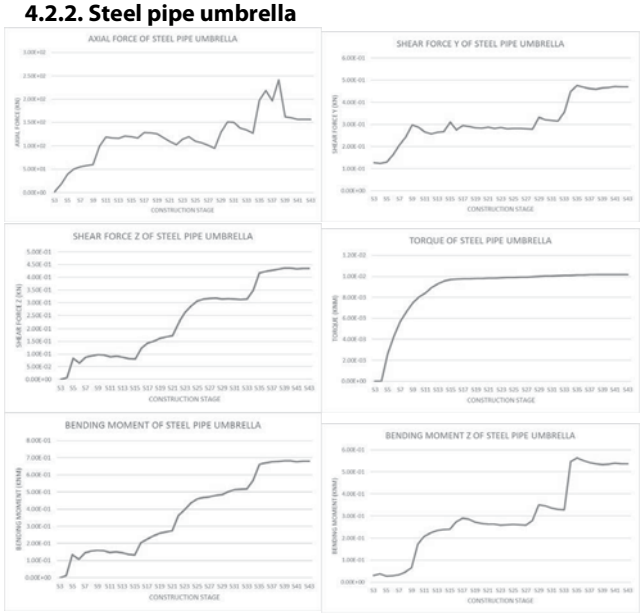

Figure 10. Forces and moment of steel pipe umbrella

Maximum axial force value of steel pipe umbrella is 241.2525 (kN) at stage 38 (S38). Maximum shear force Y value of steel pipe umbrella is 0.4763389 (kN) at stage 35 (S35). Maximum shear force Z value of steel pipe umbrella is 0.436604 (kN) at stage 39 (S39). Maximum torque value of steel pipe umbrella is 0.01018 (kNm) at stage 41 (S41). Maximum bending moment Y value of steel pipe umbrella is 0.683312 (kNm) at stage 39 (S39). Maximum bending moment Z value of steel pipe umbrella is 0.564197 (kNm) at stage 35 (S35).

4.2.2. Tunnel lining

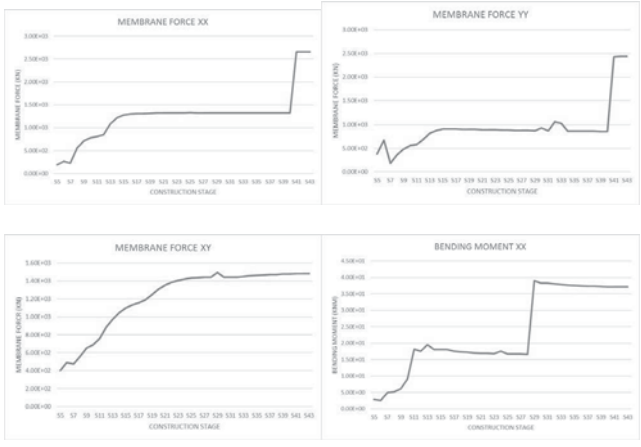

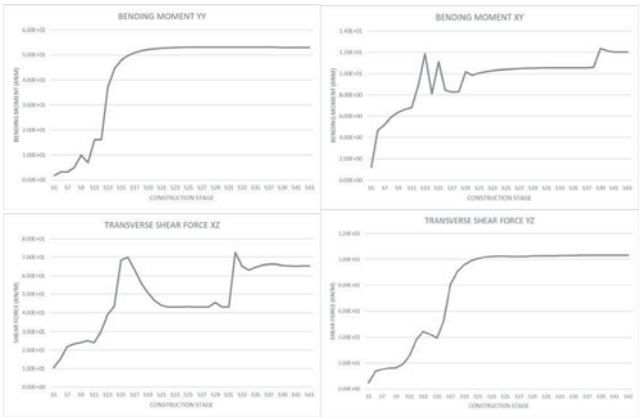

Figure 11. Forces and moment of tunnel lining

Maximum membrane force XX value of tunnel lining is 2658.403 (kN) at stage 42 (S42) and stage 43 (S43). Maximum membrane force YY value of tunnel lining is 2434.135 (kN) at stage 42 and 43 (S42 and S43). Maximum membrane force XYY value value of tunnel lining is 1496.771 (kN) at stage 29 (S29). Maximum bending moment XX value of tunnel lining is 38.98207 (kNm) at stage 29 (S29). Maximum bending moment YY value of tunnel lining is 53.17263 (kNm) at stage 26 (S26). Maximum bending moment XY value of tunnel lining is 12.35642 (kNm) at stage 39 (S39). Maximum transverse shear force XZ value of tunnel lining is 72.54777 (Kn/m) at stage 32 (S32). Maximum transverse shear force YZ value of tunnel lining is 103.3326 (Kn/m) at stage 41 (S41).

4.3. LINING STRESSES

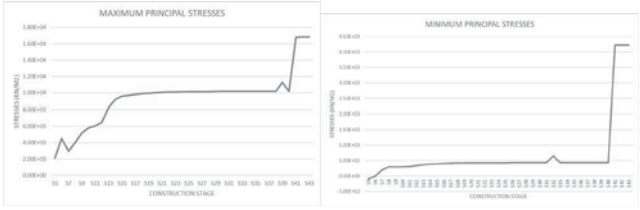

Figure 12. Maximum and minimum principal stresses on the lining

The maximum principal stresses in the lining appeared at the 43rd construction stage (S43), reaching a value of 16826.45 (kN/m2).

The maximum and minimum principal stresses on the lining change according to each construction phase. We take the construction phase with the maximum stress as the value for calculating and designing the segments.

4.4. LINING STRAINS

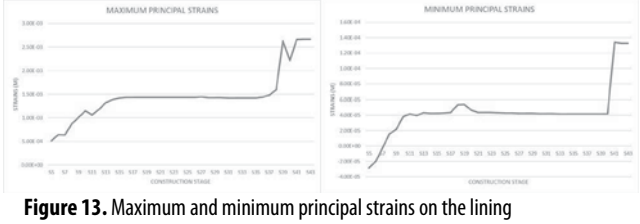

Figure 13. Maximum and minimum principal strains on the lining

Construction stages S1, S2, S3, and S4 are the initial excavation stages; stage 5 activates the tunnel lining components, so strains in the tunnel lining appear at this stage. The strains of the tunnel lining continuously change in value and location at each construction stage.

The maximum principal strains in the lining appeared at the 42nd construction stage (S42), reaching a value of 0.002662392m (=2.662392mm).

5. CONCLUSION

A series of 3-D numerical analyses were performed using the finite element with a simple linear elastic model to simulate tunnel excavations using NATM. The following conclusions may be drawn. The tunnel support lining is the most relevant single factor analyzed in reducing induced settlements. The closer to face the lining is concreted, the smaller the displacements, even if the support is not yet fully activated. Full activation with invert closure also significantly reduces induced displacements. The relation between displacement reduction and free span distance is not linear. More significant reductions were computed for shorter spans.

From the design results stated above, we can see that the maximum values of soil displacement, tunnel crown displacement, stresses, and strains of the tunnel lining and force and moment in structural members are not located on one fixed section or fixed construction stage like the 2D simulation we often do, the value and position change continuously at each construction stage, so when designing the NATM tunnels, it is necessary to simulate 3D tunnel in as much detail as possible to provide accurate and realistic data, to calculate and control risks that may occur during construction.

The previous conclusions coincide with common sense acquired empirically during years of NATM tunneling in many countries. This paper, however, gives theoretical support to many of the techniques used in NATM. Numerical analyses, in general, are a powerful tool that may help in NATM excavations by reducing uncertainties related to empirical trials during the excavation process. This approach may prove risky and costly in some instances, and numerical simulations work as reduced models that can avoid some of these trials.

REFERENCES

[1]. Beer, G., Plank, J., 1999. Austrian Research Initiative on Numerical Simulation in Tunnelling. World Tunnel Congress'99, Challenges for the 21st Century. Balkema, Oslo, Norway. pp. 13-22.

[2]. Dasari, G.R., Rawlings, C.G., Bolton, M.D., 1996. Numerical Modelling of a NATM Tunnel Construction in London Clay. Geotechnical Aspects of Underground Construction in Soft Ground. Balkema, London, UK. pp. 491–496.

[3]. Kovari, K., 1994. On the existence of the NATM: erroneous concepts behind the new Austrain tunneling method. Tunnel, 16–25

[4]. Moraes Jr. A.H., 1999. Three-dimensional numerical simulation of tunnels excavated with NATM. MSc Thesis, University of Brasilia, Brazil (in Portuguese).

[5]. Seon-Hong Kim, Ki-Lim Kim, Jung-Jin Park, Dohyun Kim. 2012. A Study on the Design Loads of Concrete Lining using Ground-Lining Interaction Model in NATM Tunnel. World Tunnel Congress. Bangkok

[6]. Aejaz Ahmad, Natasha Ahirwar, Mayank Sinha. 2019. New Austrian Tunneling Method (NATM) in Himalayan Geology: Emphasis on Execution Cycle Methodology. International Journal of Engineering Research & Technology (IJERT).

[7]. Conrad Ng, Peter Poon, Tim Leung, Lawrence Tsang. 2016. Performance of NATM Hard Rock Tunnelling for Large Span Mined Tunnel underneath Cross-Harbour Tunnel. The World Tunnel Congress WTC

[8]. M.M. de Farias, A.H. Moraes Jr and A.P. de Assis (2004), Displacement control in tunnels excavated by the NATM: 3-D numerical simulations. Tunneling and Underground Space Technology, 19, pp. 283-293.

[9]. W.S. Zhu, S.C. Li and S.C. Li (2003), Systematic numerical simulation of rock tunnel stability considering different rock conditions and construction effects. Tunneling and Underground Space Technology, 18, pp. 531-536.

[10]. K.F. Bizjak and B. Petkovsek (2004), Displacement analysis of tunnel support in soft rock around a shallow highway tunnel at Golovec. Engineering Geology, 75, pp. 89-106.